Hindawi
Journal of Chemistry
Volume 2022, Article ID 8372048, 7 pages
https://doi.org/10.1155/2022/8372048

Research Article

Spray-Dried Griseofulvin-Lactose Matrix for Enhanced Solubility Using a Spray-Drying Biochemical Process

Tian Lan,[1] Jie Yang,[2] Zhi-jie Yang,[1] and Hong-wen Wu [1]

[1]*Department of Pharmacy, Liuzhou Worker's Hospital, The Fourth Affiliated Hospital of Guangxi Medical University, Liuzhou, Guangxi 545007, China*
[2]*Department of Science and Education, Liuzhou Worker's Hospital, The Fourth Affiliated Hospital of Guangxi Medical University, Liuzhou, Guangxi 545007, China*

Correspondence should be addressed to Hong-wen Wu; dr.hongwen.wu@outlook.com

Received 21 September 2021; Revised 10 October 2021; Accepted 15 October 2021; Published 5 July 2022

Academic Editor: Weiguo Li

Griseofulvin (GF) is a hydrophobic drug with a low solubility. In order to improve the solubility of GF, which has low water solubility, this report uses the spray-drying technique to prepare complexes with lactose to promote the solubility and oral bioavailability of GF. The solution samples were spray dried using different ratios of ethanol or acetone solutions as dissolution media. By characterization of the obtained spray-dried powders, we found that the solubility of the different groups of samples obtained by spray drying was increased, and similarly, their dissolution rates were also increased to different degrees. By comparison, the greatest increase in solubility was obtained in an aqueous acetone solution, showing the greatest ability and efficiency of acetone in promoting the solubility of GF during the spray-drying process.

1. Introduction

Griseofulvin, (2S, 6′R)-7-chloro-4, 6-dimethoxybenzofuran-3-one-2-spiro-1′-(2′-methoxy-6′-methylcyclohex-2′-en- 4′-one), was primly isolated from *Penicillium griseofulvumin* 1939, and it is one of the first batches of antifungal natural drugs that were found and developed [1]. GF is widely used as an antibiotic and antifungal drug, which inhibits the growth of dermatophytes, possibly by preventing microtubulin polymerization and destroying spindle formation, thus inhibiting fungal mitosis and nucleic acid synthesis. Clinically, GF can be used as the preferred drug for tinea cephalis; meanwhile, it is suitable for treatment in toenail infections and other ringworms. There are some side effects of GF including headaches, gastrointestinal reactions, and skin rash. Since it is mainly distributed in the epidermal stratum corneum, its toxicity to humans is relatively low, so it is generally used for oral treatment of dermatitis [2, 3]. The antibacterial activity of GF is predicted through a computer aided-technique at present [4]. It was also examined that GF has potential antiviral and anticancer effects [5, 6].

GF is a hydrophobic drug with a low solubility. The solubility in the PBS as measured by Petersen et al. [7] is about 7.7(μg/mL), while in the water, measured by Thakkar et al. [8], it is about 15(μ/mL). As its effective dose is close to the limit of toxicity, the preparation of GF must be carefully designed to achieve maximum absorption. Hence, the water-insolubility characteristics of GF should be improved. In order to increase its solubility in water and improve bioavailability, not only maximum absorption of the drug is achieved but also the dose administered can be reduced and the risk of toxicity is reduced. Solubility in water has become an outstanding factor in improving the efficacy of GF. On the chemical side, changes in molecular structure have been reported to increase the solubility of GF. Amorphous solid dispersion can effectively replace the method of changing molecular structure for increasing solubility [9]. Recently, a series of preparation methods have successfully improved the solubility of GF. For instance, micro- and nano-structured GF is fixed to a silica structure [8], the solvent of GF was prepared into a new polymer dispersion [10], and taking advantage of supercritical fluid- (SCF-) assisted

atomization, we prepared micronized GF [11]. We improve the dissolution performance and bioavailability of the drug by nonionic surfactant vesicles (niosomes) [12], nanocrystalline form, and a self-emulsifying drug delivery system (sedds) [13] for oral administration.

It showed that GF can improve the dissolution behavior of amorphous solid dispersion particles by reducing the particle diameter and inhibiting its recrystallization [14]. The incorporation of surfactants and the preparation of amorphous solid dispersion by spray drying can enhance the miscibility and solubility of GF in water [15]. Through studies and comparisons, the solubility of Gleevec in ethanol and acetone was found to be quite high [16, 17]. The experiment dissolves the GF into ethanol or acetone and dissolves lactose into water, using the spray drying technique and atomizing the solution or suspensions. The small droplets are quickly dried in the high-temperature airstream to obtain fine powder [18]. In this process, spray-drying techniques transform crystalline hydrophobic drugs into amorphous morphology, and the amorphous drug loose lattice structure has good solubility in water.

The aim of the present article was to develop oral bioavailability of GF through the spray-drying technique (GF dissolved in ethanol/acetone and lactose dissolved in water in certain proportions, respectively) according to suitable parameters to obtain the dried products, and their dissolution properties and various physical and chemical characteristics were characterized.

2. Design of Spray-Drying Experiments

2.1. Preparation of the GF Solution. For each experiment, a GF solution was freshly prepared at a concentration of 2.5 mg/ml, where the solvent used for sample A was water : ethanol in the ratio of 100 : 0v/v, sample B water : ethanol in the ratio of 50 : 50v/v, and sample C water : acetone in the ratio of 50 : 50v/v. Prior to the configuration of the preceding sample solutions, 9.5g of lactose was first added to the three waters to ensure complete dissolution of the lactose and a consistent ratio of solid components in each sample. After the lactose was completely dissolved, the aqueous lactose solution was slowly poured into ethanol/acetone and then stirred thoroughly at a slow speed (100 rpm/min) to prevent the lactose from precipitating under vigorous stirring. A solution of each sample was obtained, stirred, and set aside.

2.2. Spray-Drying Process. The experimental procedure was performed using a small spray dryer (Shanghai YC-015). Spray drying was carried out at a nitrogen gas flow rate of 25 kg/h and a solution flow rate of 12 ml/min using a nozzle of 0.5 mm diameter. The three solutions were completed by three spray processes under the same conditions, respectively. The parameters of the three spray-drying processes were unchanged, fan frequency 50.0 Hz, inlet air temperature 130 ± 1°C, outlet air temperature 120 ± 3°C, and spray pressure 0.20 MPa. After the completion of the spraying process, the powder of each sample was obtained in the collection hopper, and sample B was dried at a flow rate of 12 ml/min. The samples were sealed and stored.

2.3. Characters of Samples

2.3.1. Dissolution Experiment. Separate samples of 0.35 g were compressed into tablets under the same pressure and prepared in triplicate to obtain the disintegration dissolution data. The dissolution data were obtained by using an RC1210G solubility meter (Xinzhi, China), the extraction method was the paddle method, the speed was 75 rpm/min, the temperature was 37.0 ± 0.1°C, and the sampling height was 750 mL. During the dissolution process, 1.0 ml was sampled separately using a sampling needle at the same interval, and the standard solution was replenished in time until the dissolution process was finished.

2.3.2. Ultraviolet-Visible Spectrophotometer (UV-Vis). The solution obtained from the dissolution experiment was filtered into the microporous filter membrane and configured as the required sample, and the absorbance was detected by using a UV-Vis spectrophotometer to draw the dissolution curve; we measured the maximum wavelength at 321 nm. The instrument used was a UV-2401 pc spectrophotometer, Shimadzu, Kyoto, Japan.

2.3.3. Differential Scanning Calorimetry (DSC). Thermodynamic analysis of each group of sample powders was carried out using a differential scanning calorimeter (HSC-4 DSC, Henven, China). Samples for DSC determination were prepared in sealed, curled aluminium pans according to standard procedures. Approximately 7.0 mg of each specimen was used for analysis. In the test, the samples were heated from 30°C to 350°C at a rate of 5°C/min.

2.3.4. Fourier Transform Infrared Spectroscopy (FTIR). Fourier transform infrared spectroscopy (FTIR) was used to study each group of samples and the corresponding raw materials. For preparation, KBr particles were predried, ground homogeneously, and mixed with each sample powder, pressed into transparent sheets, and placed in a mold, which were scanned in a Nicolet 6700 FTIR spectrometer (Thermo Fisher Scientific).

2.3.5. Scanning Electron Microscopy (SEM). The sample powder was uniformly coated with gold, and subsequently, the sample was placed on an aluminum sample peg with a carbon tape. The gold-plated samples were examined with a JSM-7200F scanning electron microscope (SEM, JEOL Ltd.).

2.3.6. Thermogravimetric Analyzer (TGA). Samples were analyzed using a thermogravimetric analyzer (TGA Q5000 V3.17 Build 265). In this process, N2 is used as an equilibrium gas. The temperature during thermogravimetric examination is 35–350°C, and the heating rate is 5°C/min. The sample is placed in an alumina pan to be examined.

2.3.7. N2 Adsorption. Mesoporous adsorption experiments were performed on the powder samples separately to evaluate the differences in pore size distribution, surface area, and pore volume of the different samples.

2.3.8. X-Ray Diffraction (XRD). The powder samples were studied by XRD analysis using a Siemens D5000 diffractometer to investigate the compositional similarities and differences.

3. Results and Disscusion

The solutions obtained from the dissolution experiments were passed through a 0.22 μm filter membrane and diluted at the same multiples to obtain test samples. The absorbance was measured with a pc UV-Vis spectrophotometer UV-2401, and the dissolution curves were plotted as shown in Figure 1. For the physical mixture, the solubility of GF in water was low, and after the spray drying treatment, the solubility and dissolution rate of both groups of powders increased. Comparing sample A and sample B, we found that the solubility of GF was significantly higher in sample B, but the dissolution rate was smaller than that of s3ample A and it took more time to reach dissolution equilibrium. This may be due to the greater proportion of GF dissolved in acetone at the same solid-to-liquid ratio and the fact that more of the GF crystal structure was disrupted during the spray drying process, resulting in a large amount of amorphous solid GF, leading to a significant increase in its solubility. Similarly, in this process, due to the lower solubility of lactose in acetone, more lactose crystals precipitate prior to the high-temperature drying process and the proportion of amorphous lactose is reduced, making the whole system more difficult to break down and dissolve. Various facts show that the amorphous form of GF after dissolution in organic solvents and after the spray-drying process increases the solubility of GF in water considerably.

We measured the IR spectra of raw materials, physical mixtures, and spray-dried samples, as shown in Figure 2. The absorption peaks of the raw material lactose and GF at all wavelengths were present in the physical mixture. For the spray-dried sample, most of its sharp absorption peaks disappeared and merged into flat, blunt absorption peaks, with reduced density and strength of hydrogen bonds and reduced crystallinity, indicating the appearance of amorphous products, whether ethanol or acetone was used as the solvent. Sample B has a smoother peak in the GF characteristic peak region than sample A, indicating the generation of more amorphous GF.

We performed thermal analysis for each raw material and spray-dried samples. By analyzing the DSC curves of the samples (Figure 3), the heat absorption peaks of crystalline water and lactose crystals of lactose appeared at 148°C and 209°C, respectively, while the heat absorption peak of GF appeared at 220°C. In the physical mixture, the position and peak shape of the heat absorption peak of lactose remained basically unchanged. The heat absorption peak of melting GF crystals moved to the low-temperature region to 215°C, which may be when the less content reduced its melting heat absorption time, resulting in narrowing of the peak width and shift of the peak top position to the low-temperature region. For sample B, the residual acetone boiling point is lower than that of ethanol, which shifts the peak position to the low-temperature region relative to sample A. The heat

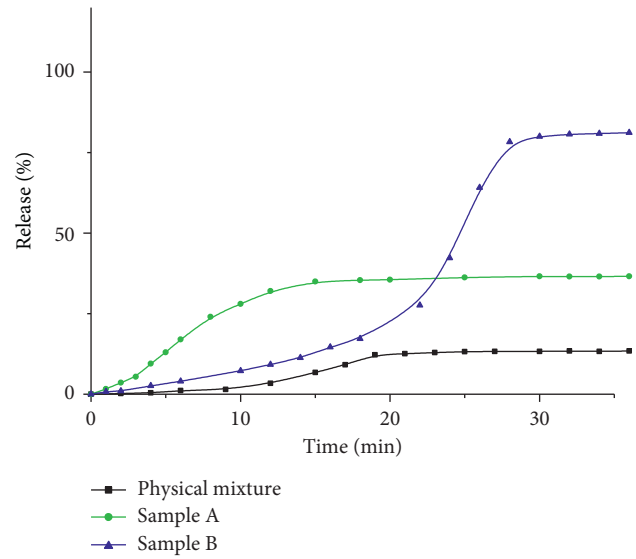

Figure 1: Release spectra of GF tablets in the two samples and physical mixture.

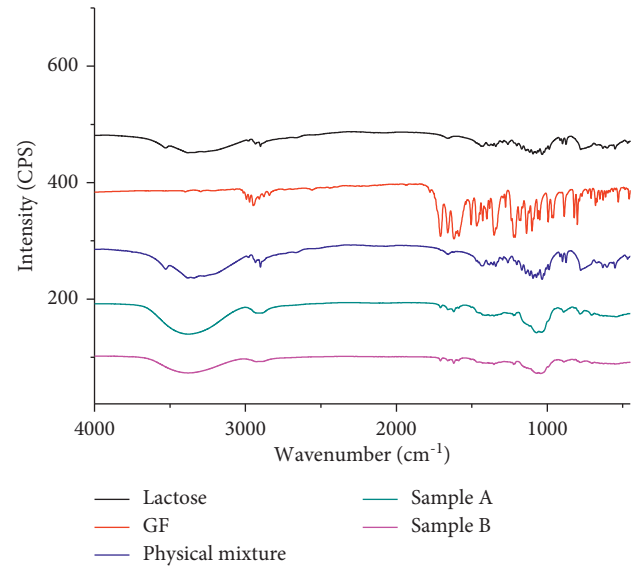

Figure 2: FTIR spectra of the raw materials, physical mixture, and samples.

absorption peak similar to that of lactose crystalline water at 130–140°C is larger and higher than that of sample B in the TGA curve (Figure 4), and both samples showed the same weight loss trend. However, the derivative weight loss curves suggest that sample B may have a more complex crystalline/noncrystalline structure.

According to the XRD curves (Figure 5), the α-lactose peaks in both samples were 12.5°, 19.1°, 19.6°, and 19.9° at 2θ, respectively, and the peaks of β-lactose at $2\theta = 10.5°$ were absent in both samples, suggesting that both ethanol and acetone can inhibit the variable-spin behavior of lactose to some extent [19, 20]. In the interval 5–45°, the peak positions of the two samples were basically the same, but the lactose peak of sample B was significantly sharper and steeper than

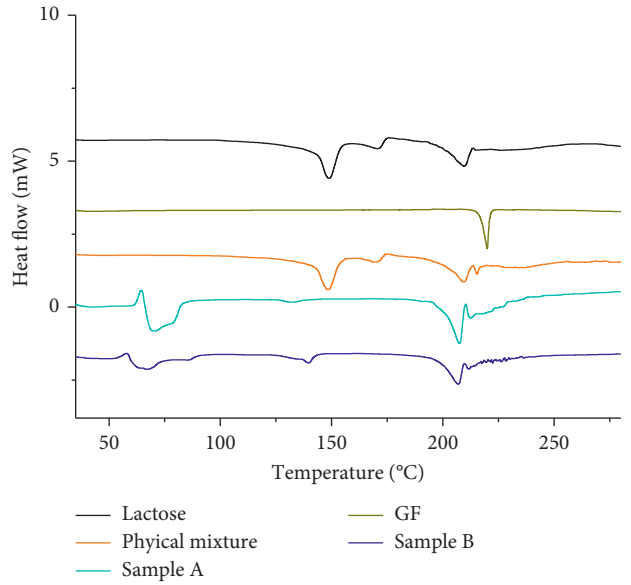

Figure 3: DSC curves of the raw materials, physical mixture, and samples.

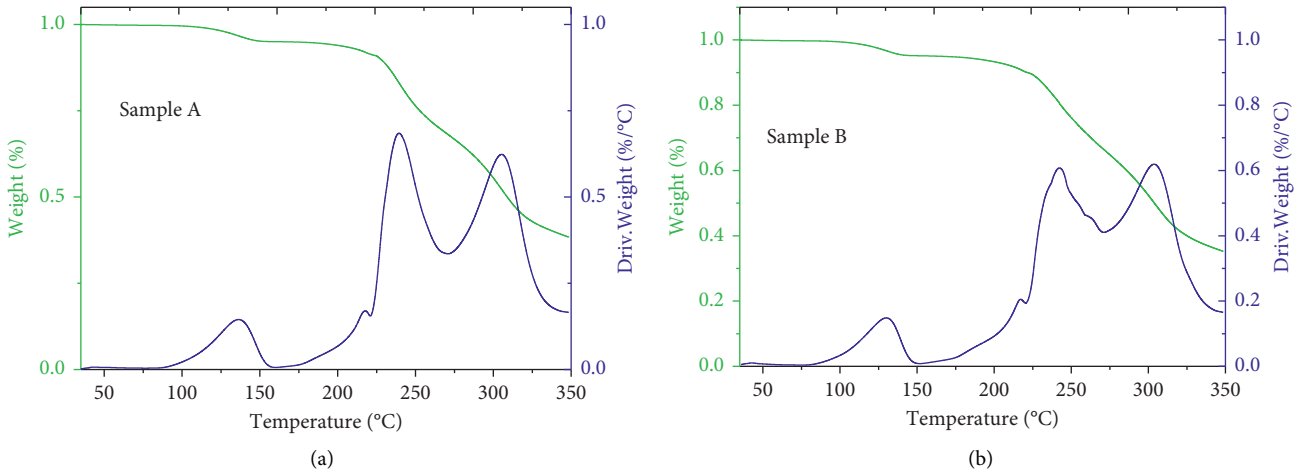

Figure 4: The TGA curves of the two spray-dried samples.

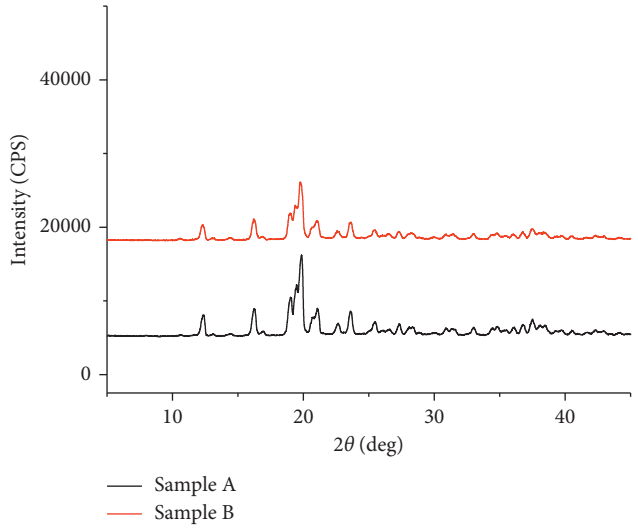

Figure 5: XRD curves of the two spray-dried powders.

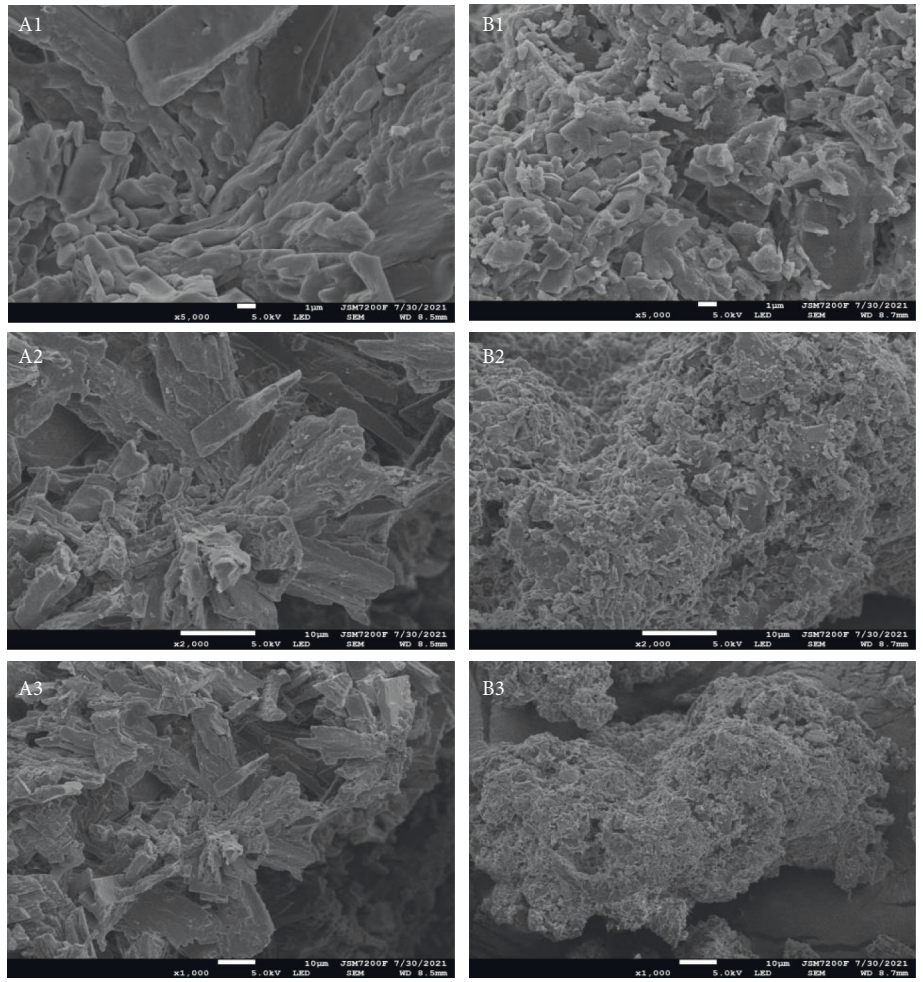

Figure 6: SEM images of the two spray-dried powders in 5000x, 2000, and 1000, respectively (A1–3 for sample A; B1–3 for sample B).

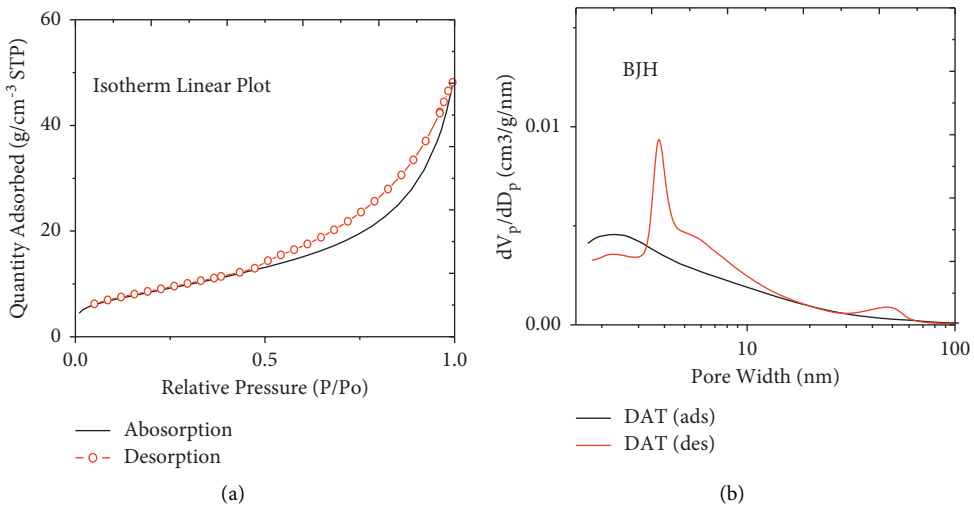

Figure 7: The nitrogen adsorption curve. Isotherm linear plot (a) and BJH adsorption dV/dlog (w) pore volume (b) of sample B.

that of sample A, suggesting the production of more amorphous lactose, which was consistent with the dissolution curves. This can also be observed in the SEM image (Figure 6).

Sample A and sample B exhibit completely different states in the field of view of SEM (Figure 6). Sample A is a lamellar structured aggregate with a smooth surface; sample B exhibits porous aggregates of various fine crystal particles.

The two fields of view indicate different crystalline/non-crystalline states, suggesting that most of the lactose in sample A may be present in an amorphous form. For sample B in the porous state, we performed a nitrogen adsorption experiment to calculate and evaluate its pore structure (Figure 7). Its BET adsorption and desorption curves visually represent its porous nature. The average pore size was calculated by analysis to be about 8.7 nm, cumulative volume of pores between 1.7000 nm and 300.0000 nm width: 0.073814 cm^3/g, and its large pore volume may provide its better compressibility.

4. Conclusions

The solubilisation of insoluble drugs GF is a simple and practical study. In this experiment, we spray-dried GF with ethanol and acetone as dispersion media, respectively, and solubilisation was achieved with both solvents, with a 5–10-fold increase in the solubility of GF after the experimental manipulation. Moreover, the solubilisation efficiency of GF was higher with acetone than with ethanol. Interestingly, the different solvents also had different effects on the properties of the spray-dried excipient lactose. This may provide ideas for programmed manipulation of the solubilisation of insoluble drugs and modulation of their solubilisation behaviour.

Data Availability

The data used to support the findings of this study are included within the article.

Conflicts of Interest

The authors declare no conflicts of interest.

Acknowledgments

The work was supported by Liuzhou Worker's Hospital (The Fourth-Affiliated Hospital of Guangxi Medical University). The authors performed the spray drying and instrumental analysis in Hunan Yaxiang Pharma Co. Pty. The authors thank Bo Wang from Hunan Yaxiang Pharma Co. Pty. for his assistance in spray drying and instrumental analysis. For enquiry of production and analysis, contact Hunan Yaxiang Pharma Co. Pty. via 252856756@qq.com.

References

[1] A. B. Petersen, M. H. Rønnest, T. O. Larsen, and M. H. Clausen, "The chemistry of griseofulvin," *Chemical Reviews*, vol. 114, no. 24, pp. 12088–12107, 2014.

[2] L. De Carli and L. Larizza, "Griseofulvin," *Mutation Research: Reviews in Genetic Toxicology*, vol. 195, no. 2, pp. 91–126, 1988.

[3] V. Kartsev, A. Geronikaki, A. Petrou et al., "Griseofulvin derivatives: synthesis, molecular docking and biological evaluation," *Current Topics in Medicinal Chemistry*, vol. 19, no. 13, pp. 1145–1161, 2019.

[4] A. Geronikaki, V. Kartsev, A. Petrou et al., "Antibacterial activity of griseofulvin analogues as an example of drug repurposing," *International Journal of Antimicrobial Agents*, vol. 55, no. 3, Article ID 105884, 2020.

[5] N. D. Paguigan, M. H. Al-Huniti, H. A. Raja et al., "Chemoselective fluorination and chemoinformatic analysis of griseofulvin: natural vs fluorinated fungal metabolites," *Bioorganic & Medicinal Chemistry*, vol. 25, no. 20, pp. 5238–5246, 2017.

[6] T. Oda, "Effects of 2′-demethoxy-2′-propoxygriseofulvin on microtubule distribution in Chinese hamster V79 cells," *Journal of Antibiotics*, vol. 59, no. 2, pp. 114–116, 2006.

[7] A. B. Petersen, G. Konotop, N. H. M. Hanafiah et al., "Strategies for improving the solubility and metabolic stability of griseofulvin analogues," *European Journal of Medicinal Chemistry*, vol. 116, pp. 210–215, 2016.

[8] M. Thakkar, M. S. Islam, A. Railkar, and S. Mitra, "Antisolvent precipitative immobilization of micro and nanostructured griseofulvin on laboratory cultured diatom frustules for enhanced aqueous dissolution," *Colloids and Surfaces B: Biointerfaces*, vol. 196, Article ID 111308, 2020.

[9] S. Baghel, H. Cathcart, and N. J. O'Reilly, "Polymeric amorphous solid dispersions: a review of amorphization, crystallization, stabilization, solid-state characterization, and aqueous solubilization of biopharmaceutical classification system class II drugs," *Journal of Pharmaceutical Sciences*, vol. 105, no. 9, pp. 2527–2544, 2016.

[10] H. Al-Obaidi, R. M. Kowalczyk, R. Kalgudi, and M. G. Zariwala, "Griseofulvin solvate solid dispersions with synergistic effect against fungal biofilms," *Colloids and Surfaces B: Biointerfaces*, vol. 184, Article ID 110540, 2019.

[11] E. Reverchon, G. D. Porta, A. Spada, and A. Antonacci, "Griseofulvin micronization and dissolution rate improvement by supercritical assisted atomization," *Journal of Pharmacy and Pharmacology*, vol. 56, no. 11, pp. 1379–1387, 2010.

[12] P. S. Jadon, V. Gajbhiye, R. S. Jadon, K. R. Gajbhiye, and N. Ganesh, "Enhanced oral bioavailability of griseofulvin via niosomes," *AAPS PharmSciTech*, vol. 10, no. 4, pp. 1186–1192, 2009.

[13] A. I. Arida, M. M. Al-Tabakha, and H. A. J. Hamoury, "Improving the high variable bioavailability of griseofulvin by SEDDS," *Chemical and Pharmaceutical Bulletin*, vol. 55, no. 12, pp. 1713–1719, 2007.

[14] K. Zheng, Z. Lin, M. Capece, K. Kunnath, L. Chen, and R. N. Davé, "Effect of particle size and polymer loading on dissolution behavior of amorphous griseofulvin powder," *Journal of Pharmaceutical Sciences*, vol. 108, no. 1, pp. 234–242, 2019.

[15] A. Bhanderi, F. Bari, and H. Al-Obaidi, "Evaluation of the impact of surfactants on miscibility of griseofulvin in spray dried amorphous solid dispersions," *Journal of Drug Delivery Science and Technology*, vol. 64, Article ID 102606, 2021.

[16] S. Zhao, Y. Ma, J. Gong, B. Hou, and W. Tang, "Solid-liquid phase equilibrium and thermodynamic analysis of griseofulvin in twelve mono-solvents," *Journal of Molecular Liquids*, vol. 296, Article ID 111861, 2019.

[17] X. Zhao, A. Farajtabar, G. Han, and H. Zhao, "Griseofulvin dissolved in binary aqueous co-solvent mixtures of N, N-dimethylformamide, methanol, ethanol, acetonitrile and N-methylpyrrolidone: solubility determination and thermodynamic studies," *The Journal of Chemical Thermodynamics*, vol. 151, Article ID 106250, 2020.

[18] B. Wang, F. Liu, J. Xiang et al., "A critical review of spray-dried amorphous pharmaceuticals: synthesis, analysis and application," *International Journal of Pharmaceutics*, vol. 594, Article ID 120165, 2021.

[19] S. Tan, T. Jiang, A. Ebrahimi, and T. Langrish, "Effect of spray-drying temperature on the formation of flower-like lactose for griseofulvin loading," *European Journal of Pharmaceutical Sciences*, vol. 111, pp. 534–539, 2018.

[20] B. Wang, H. Li, J. Xiang, J. Zheng, and J. Wang, "Fabrication of agglomerated lactose using fluidized bed for good compressibility," *Journal of Nanomaterials*, vol. 2021, Article ID 9918847, 6 pages, 2021.